IOPscience iopscience.iop.org

Home Search Collections Journals About Contact us My IOPscience

Preliminary reliability test of lateral-current-injection GaInAsP/InP membrane distributed feedback laser on Si substrate fabricated by adhesive wafer bonding

This content has been downloaded from IOPscience. Please scroll down to see the full text.

2017 Jpn. J. Appl. Phys. 56 028002

(http://iopscience.iop.org/1347-4065/56/2/028002)

View the table of contents for this issue, or go to the journal homepage for more

Download details:

IP Address: 131.112.10.178
This content was downloaded on 19/07/2017 at 18:14

Please note that terms and conditions apply.

You may also be interested in:

Room-temperature continuous-wave operation of GaInAsP/InP lateral-current-injection membrane laser bonded on Si substrate
Daisuke Inoue, Jieun Lee, Kyohei Doi et al.

Thermal properties of lateral-current-injection semiconductor membrane Fabry–Perot laser under continuous-wave operation
Takuo Hiratani, Kyohei Doi, Jieun Lee et al.

High-differential quantum efficiency operation of GaInAsP/InP membrane distributed-reflector laser on Si
Takahiro Tomiyasu, Takuo Hiratani, Daisuke Inoue et al.

Waveguide loss reduction of lateral-current-injection type GaInAsP/InP membrane Fabry–Pérot laser
Takahiro Tomiyasu, Takuo Hiratani, Daisuke Inoue et al.

Room-temperature continuous-wave operation of membrane distributed-reflector laser
Takuo Hiratani, Daisuke Inoue, Takahiro Tomiyasu et al.

Low-threshold-current operation of membrane distributed-feedback laser with surface grating bonded on Si substrate
Yuki Atsuji, Kyohei Doi, Takuo Hiratani et al.

90 °C continuous-wave operation of GaInAsP/InP membrane distributed-reflector laser on Si substrate
Takuo Hiratani, Daisuke Inoue, Takahiro Tomiyasu et al.

Reliable Operation of GaInAsP/InP Distributed Feedback Laser with Wirelike Active Regions
Kazuya Ohira, Nobuhiro Nunoya, Hideki Yagi et al.

Japanese Journal of Applied Physics **56**, 028002 (2017)
https://doi.org/10.7567/JJAP.56.028002

BRIEF NOTE

Preliminary reliability test of lateral-current-injection GaInAsP/InP membrane distributed feedback laser on Si substrate fabricated by adhesive wafer bonding

Kai Fukuda[1], Daisuke Inoue[1], Takuo Hiratani[1], Tomohiro Amemiya[1,2], Nobuhiko Nishiyama[1,2], and Shigehisa Arai[1,2*]

[1]*Department of Electrical and Electronic Engineering, Tokyo Institute of Technology, Meguro, Tokyo 152-8552, Japan*
[2]*Institute of Innovative Research (IIR), Tokyo Institute of Technology, Meguro, Tokyo 152-8552, Japan*

*E-mail: arai@pe.titech.ac.jp

Received August 23, 2016; accepted November 24, 2016; published online January 10, 2017

A preliminary reliability test was performed for lateral-current-injection GaInAsP/InP membrane Distributed Feedback (DFB) lasers fabricated by multi-regrowth and adhesive wafer bonding. The measurement was conducted for lasers with two different types of p-side electrode: Ti/Au and Au/Zn/Au. The device with the Au/Zn/Au electrode, which had better current–voltage (*I*–*V*) characteristics, showed no degradation of differential quantum efficiency and threshold current after continuous aging for 310 h at a bias current density of 5 kA/cm^2. This result indicates that the multi-regrowth and bonding process for the GaInAsP/InP membrane DFB laser will not impact the initial reliability.
© 2017 The Japan Society of Applied Physics

On-chip optical interconnection technology has emerged as one of the solutions for electrical interconnection problems such as Joule heating and signal delay in Si large-scale-integrated circuits.[1] Ultra-low power consumption lasers fabricated on Si are needed as a light source for this technology, and thus this is an attractive field of research. There are several reports of lasing characteristics under room-temperature continuous-wave (RT-CW) operation[2] and direct modulation[3] of semiconductor lasers on Si. The reliabilities of lasers on Si fabricated by plasma activated bonding[4] and direct growth of quantum dot active layers[5] have been reported in addition to their static and dynamic characteristics. However, conventional lasers consisting of semiconductor cladding layers are not sufficient for use as the light source for on-chip optical interconnection in terms of power consumption, because optical confinement to the active layer is not strong. In contrast, a membrane DFB laser, which consists of a thin (<300 nm) semiconductor core and dielectric cladding layers, was proposed and very low threshold RT-CW operation was demonstrated under an optical pump[6–9] and current injection[10,11] using a lateral-current-injection (LCI) structure.[12] An integration of a membrane DFB laser with passive waveguides and photodiodes was realized by a butt-jointed built-in (BJB) structure,[13] and RT-CW operation of the LCI membrane DFB laser with low threshold current (<0.5 mA) was reported.[14,15] Although the fundamental characteristics of the membrane DFB laser were confirmed, its reliability was not previously reported. In addition, our previous device displayed poor electrical characteristics.[15] The fabrication process through three-steps regrowth by organometallic vapor-phase-epitaxy (OMVPE) and adhesive bonding has the possibility to degrade the reliability of the laser. In addition, there are no reports on the reliability of an LCI structure or lasers fabricated by BCB adhesive bonding.

In this brief note, we report the results of an aging test of 1.55 μm wavelength membrane GaInAsP/InP DFB lasers on Si measured at room temperature (20 °C).

Figure 1 shows a schematic diagram of the membrane DFB laser. The overall fabrication procedure is described in Ref. 15. A 270-nm-thick semiconductor membrane layer with a SiO_2 cladding layer was bonded to a Si wafer by a BCB adhesive layer. The active layer consists of GaInAsP containing five strain-compensated quantum wells. The BJB waveguide was integrated to the DFB laser.

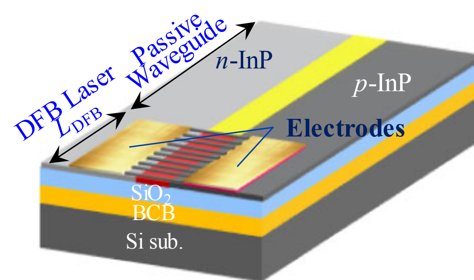

Fig. 1. (Color online) Schematic diagram of the membrane DFB laser.

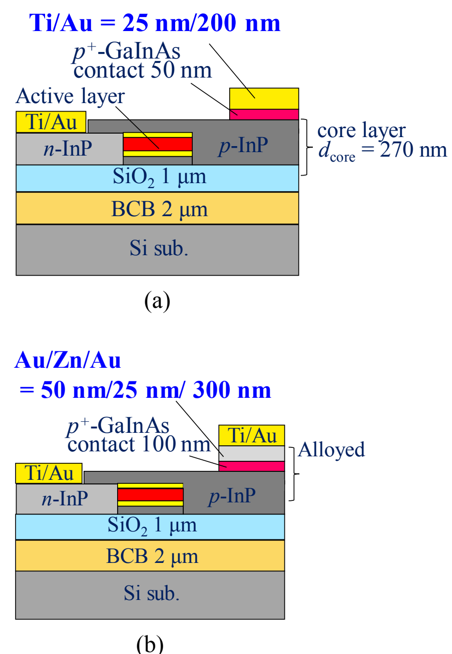

Fig. 2. (Color online) Cross sectional views of (a) Ti/Au electrode device and (b) Au/Zn/Au electrode device.

Figure 2(a) shows a cross sectional image of the membrane DFB laser in Ref. 15. The electrode metal for both n- and p-InP side contacts was Ti/Au of 25 nm/200 nm deposited by electron beam evaporation. We found that the poor electrical characteristics of our previous device were attributed to the unintentional n-type doping spike at the regrowth interface owing to surface contamination, as explained later. For this reason, an Au/Zn/Au alloyed electrode

© 2017 The Japan Society of Applied Physics

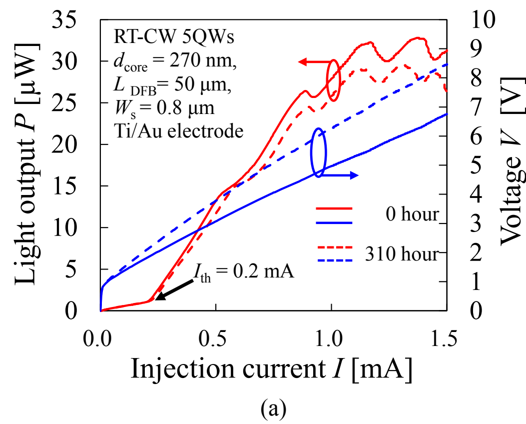

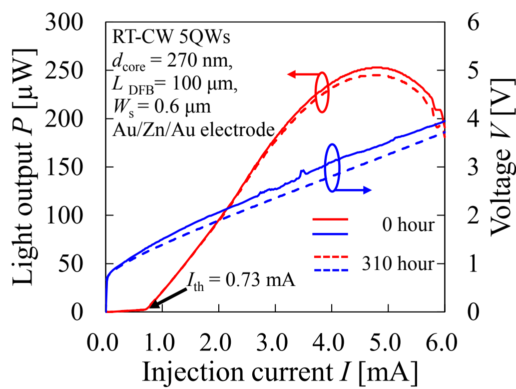

Fig. 3. (Color online) Light output and voltage characteristics before and after 310 h aging test of (a) Ti/Au electrode device and (b) Au/Zn/Au electrode device.

was introduced in order to obtain good characteristics at the p-side by using an alloying layer (counter doping by Zn diffusion) as shown in Fig. 2(b). Thermal evaporation was used to deposit Au/Zn/Au of 50 nm/25 nm/300 nm. The deposited metal was annealed in ambient N_2 by rapid thermal annealing at 350 °C for 1 min.

The aging test was performed for the two devices with the Ti/Au and Au/Zn/Au p-side electrodes under CW conditions at 20 °C. The laser chips were directly mounted on a heat sink in ambient air. The temperature of the heat sink was controlled by a thermo-electric cooler. The bias current was injected by contacting the electrode using needle probes. The measurement was conducted under constant current conditions. The Ti/Au electrode device (cavity length L_{DFB} = 50 μm, threshold current I_{th} = 0.2 mA, with passive waveguides for output at both sides) and the Au/Zn/Au electrode device (cavity length L_{DFB} = 100 μm, threshold current I_{th} = 0.73 mA, one output had a passive waveguide and the other side was a cleaved facet) were biased with current densities J_{th} of 2.5 kA/cm^2 (1 mA) and 5.0 kA/cm^2 (3 mA), respectively. The bias current density was set to as high a current as possible without thermal roll-off of output power occurring. Figures 3(a) and 3(b) show *L–I–V* curves of Ti/Au and Au/Zn/Au electrode devices, respectively, where solid lines indicate those before the aging test and dashed lines indicate those after aging test. As can be seen, the threshold currents of both devices were not degraded. As for the Ti/Au device, the drive voltage was increased and the external differential quantum efficiency was decreased from 5.4 to 4.8% after

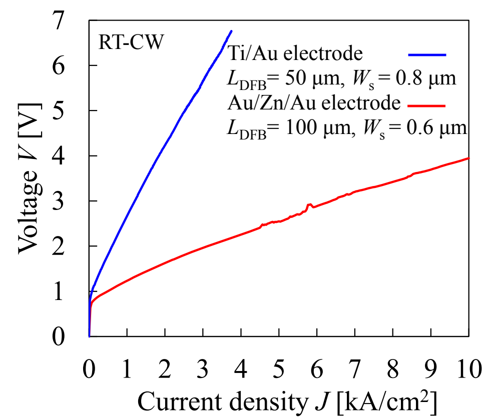

Fig. 4. (Color online) Comparison of current versus voltage characteristics between the devices with different p-side electrode metal.

the aging. The Au/Zn/Au device showed a slight decrease of voltage and no degradation of the external differential quantum efficiency. In addition, the output power did not vary up to the thermal roll-off region. The detailed results of the preliminary reliability test are described later.

Figure 4 shows a comparison of *I–V* characteristics between the devices with two different p-side electrodes. Current density was chosen as the *x*-axis because these devices had different cavity lengths. The differential resistance of the Au/Zn/Au electrode device was approximately 1/5 that of the Ti/Au electrode device. In addition, the specific contact resistance of the Au/Zn/Au electrode device was measured to be 3.2×10^{-6} Ω·cm^2 from transmission line model (TLM) measurements, while it was 5.4×10^{-3} Ω·cm^2 for the Ti/Au electrode device. Secondary ion mass spectrometry (SIMS) performed on the substrate after p-InP regrowth showed Si atoms, which acted as n-type dopant, at the interface between the contact p^{++}-GaInAs layer and regrown p-InP. The sources of the Si atoms were considered to be surface treatment before regrowth or contamination of the OMVPE reactor.[16] The *I–V* characteristics of the Au/Zn/Au electrode device were improved by the diffusion effect of the semiconductor and metal species during the annealing process.[17]

Figure 5 shows the relative light output power normalized by the initial output power of the two DFB lasers during the aging test. This aging time was sufficient to observe the rapid degradation of lasers.[18–20] The light output of the Ti/Au electrode device decreased to 89% of the initial value after 310 h. The degradation of the light output P can be approximated by the following relationship,[21]

$$P = P_0 \exp\left(-\frac{t}{T}\right),$$

where P_0 is the initial value of the light output, t is the aging time, and T is a fitting constant. The fitting results gave an estimation of T for the Ti/Au device of 3310 h. By contrast, the Au/Zn/Au electrode device showed no significant degradation in light output up to 310 h, even though higher bias current density than the Ti/Au electrode device was applied. The fluctuation in light output was within 1% during the measurement. The time constant T for the Au/Zn/Au electrode device could not be defined because degradation was not observed. It is well known that Au/Zn/Au electrodes cause faster degradation of contacts than Ti/Au electrodes

 © 2017 The Japan Society of Applied Physics

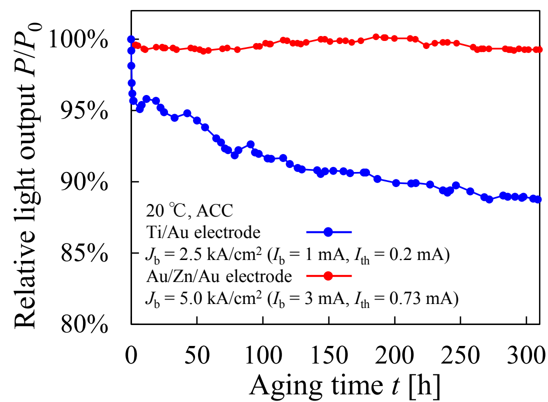

Fig. 5. (Color online) Aging characteristics of the light output normalized by initial values.

owing to Au diffusion into the semiconductor.[22] However, the membrane structure has lateral current injection, which gives a different diffusion profile compared with conventional vertical injection type lasers. This had a major impact on the reliability of the membrane DFB laser in this work.

In conclusion, we performed preliminary measurements of the reliability of an LCI-membrane DFB laser bonded on a Si substrate. The device with a p-side Au/Zn/Au electrode had better voltage characteristics than the device with a Ti/Au p-side electrode device, and showed reliable operation up to 310 h. The membrane DFB laser fabricated by multi-regrowth and BCB bonding showed no tendency of degradation of threshold current during the aging test.

Acknowledgments The authors would like to thank Professors S. Akiba, T. Mizumoto, M. Asada, Y. Miyamoto, M. Watanabe, and Y. Shoji of the Tokyo Institute of Technology for their fruitful discussions. This work was supported by JSPS KAKENHI Grant Numbers 15H05763, 25709026, 15J04654, 15J11776, and 16H06082.

1) D. A. B. Miller, Proc. IEEE **97**, 1166 (2009).
2) A. W. Fang, H. Park, O. Cohen, R. Jones, M. J. Paniccia, and J. E. Bowers, Opt. Express **14**, 9203 (2006).
3) C. Zhang, S. Srinivasan, Y. Tang, M. J. R. Heck, M. L. Davenport, and J. E. Bowers, Opt. Express **22**, 10202 (2014).
4) S. Srinivasan, N. Julian, J. Peters, D. Liang, and J. E. Bowers, IEEE J. Sel. Top. Quantum Electron. **19**, 1501305 (2013).
5) A. Y. Liu, R. W. Herrick, O. Ueda, P. M. Petroff, A. C. Gossard, and J. E. Bowers, IEEE J. Sel. Top. Quantum Electron. **21**, 1900708 (2015).
6) T. Okamoto, N. Nunoya, Y. Onodera, S. Tamura, and S. Arai, Electron. Lett. **38**, 1444 (2002).
7) T. Okamoto, N. Nunoya, Y. Onodera, T. Yamazaki, S. Tamura, and S. Arai, IEEE J. Sel. Top. Quantum Electron. **9**, 1361 (2003).
8) S. Sakamoto, T. Okamoto, T. Yamazaki, S. Tamura, and S. Arai, IEEE J. Sel. Top. Quantum Electron. **11**, 1174 (2005).
9) S. Sakamoto, H. Naitoh, H. Kawashima, M. Ohtake, Y. Nishimoto, S. Tamura, T. Maruyama, N. Nishiyama, and S. Arai, IEEE J. Sel. Top. Quantum Electron. **13**, 1135 (2007).
10) D. Inoue, J. Lee, K. Doi, T. Hiratani, Y. Atsuji, T. Amemiya, N. Nishiyama, and S. Arai, Appl. Phys. Express **7**, 072701 (2014).
11) T. Hiratani, K. Doi, J. Lee, D. Inoue, T. Amemiya, N. Nishiyama, and S. Arai, Jpn. J. Appl. Phys. **54**, 042701 (2015).
12) K. Oe, Y. Noguchi, and C. Caneau, IEEE Photonics Technol. Lett. **6**, 479 (1994).
13) D. Inoue, T. Hiratani, Y. Atsuji, T. Tomiyasu, T. Amemiya, N. Nishiyama, and S. Arai, IEEE J. Sel. Top. Quantum Electron. **21**, 1502907 (2015).
14) Y. Atsuji, K. Doi, T. Hiratani, D. Inoue, J. Lee, Y. Atsumi, T. Amemiya, N. Nishiyama, and S. Arai, Jpn. J. Appl. Phys. **54**, 080301 (2015).
15) D. Inoue, J. Lee, T. Hiratani, Y. Atsuji, T. Amemiya, N. Nishiyama, and S. Arai, Opt. Express **23**, 7771 (2015).
16) D. G. Knight, G. Kelly, J. Hu, S. P. Watkins, and M. L. W. Thewalt, J. Cryst. Growth **182**, 23 (1997).
17) A. Yamaguchi, I. Tonai, H. Okuda, N. Yamabayashi, and M. Shibata, Bunseki Kagaku **40**, 741 (1991).
18) K. Endo, S. Matsumoto, H. Kawano, I. Sakuma, and T. Kamejima, Appl. Phys. Lett. **40**, 921 (1982).
19) E. Omura, H. Uesugi, T. Kimura, Y. Kawama, and H. Namizaki, Electron. Lett. **25**, 1718 (1989).
20) T. Yamada, M. Tachikawa, T. Sasaki, H. Mori, Y. Katoda, and M. Yamamoto, Electron. Lett. **31**, 455 (1995).
21) O. Ueda, *Reliability and Degradation of III–V Optical Devices* (Artech House, Boston, MA, 1996).
22) M. Fukuda, J. Lightwave Technol. **6**, 1488 (1988).

 © 2017 The Japan Society of Applied Physics